Mutually Dispersive Pulse Coding to Enhance Non-Linear Ambiguity Suppression

John Kurian, Michael A. Temple, and Matthew J. Papaphotis
Department of Electrical and Computer Engineering
Air Force Institute of Technology, Wright-Patterson AFB, OH, USA

William M. Brown
Sensors Directorate, Air Force Research Laboratory
Wright-Patterson AFB, OH, USA

***Abstract*— Results from design, synthesis, and analysis of optimal mutually dispersive symbols are presented as an improvement over existing symbol sets employed in Non-linear Ambiguity Suppression (NLAS). A recently proposed theorem formulates the existence of symbol families having optimal mutual dispersion, a highly desirable property for NLAS applications. Results from theorem analysis are presented and compared to other suitable NLAS symbol sets, showing significant improvement in mutual dispersion characteristics. NLAS ambiguity suppression effectiveness is demonstrated using a set of optimal mutually dispersive symbols.**

I. INTRODUCTION

Radars employing pulsed waveforms are inherently ambiguous in range and Doppler. In 1962 Palermo [1] used two conjugate linear frequency modulated (LFM) pulses to demonstrate a Non-linear Ambiguity Suppression (NLAS) signal processing technique for reducing ambiguous energy in processed radar returns. The use of conjugate LFM pulses for diverse pulse coding does not extend to larger symbol families and thus has severe limitations for M-channel (M > 2) NLAS applications. Desirable NLAS symbol sets posses 1) large partial period autocorrelation peaks with low integrated sidelobe levels and 2) maximum signal dispersion when cross-correlating pulse codes within the family [2]. Symbol sets comprised of pseudo-random discrete codes, such as Gold codes, exhibit mutual dispersion properties [3] but are not optimum for NLAS. A root mean square (rms) time duration metric of correlation functions is introduced to formulate a process for obtaining optimal mutually dispersive NLAS symbols for arbitrary code family sizes [4].

II. SYMBOL DESIGN

The discovery of symbol families having desirable characteristics for NLAS applications is by no means a recent achievement. Code Division Multiple Access (CDMA) communication schemes use discrete codes exhibiting desirable properties for NLAS [3]. The search for optimal symbol sets has historically focused on discrete codes; an avenue of research not yet providing an optimal solution. Using rms time duration of correlation functions as the metric for optimality, the search for mutually dispersive codes begins by considering a pulse coded radar signal given by:

$$x(t) = \sum_{k=0}^{M-1} f_k\left(t - kT\right) \tag{1}$$

where T is the Pulse Repetition Interval (PRI) and $f_k(t)$ has a Fourier transform of the form:

$$F_k(\omega) = \sqrt{A(\omega)}\, e^{\,j\Phi_k(\omega)} \qquad A(\omega), \Phi_k(\omega) \in \Re \tag{2}$$

The processed pulse return is represented as follows:

$$\begin{aligned} F_l(\omega)H_k(\omega) &= F_l(\omega)F_k^*(\omega) \overset{\Delta}{=} P_{lk}(\omega) \\ &= A(\omega)e^{j[\Phi_l(\omega)-\Phi_k(\omega)]} \end{aligned} \tag{3}$$

When $k = l$, the processed output represents a matched filter response whose inverse Fourier transform is the signal autocorrelation function (ACF), $\rho_{kk}(t)$ given by:

$$P_{kk}(\omega) \overset{\Im^{-1}}{\Rightarrow} \rho_{kk}(t) \tag{4}$$

The NLAS process requires the ACF to be as compressed (impulse-like) as possible and the crosscorrelation function (CCF) (mismatched filter response) to be as dispersed (flat) as possible. The rms time duration of correlation functions, σ_{lk} as defined in (5a), is used to quantify correlative dispersion [5]. This definition of σ_{lk} assumes $\rho_{lk}(t)$ is normalized to unity energy with zero mean; the dot operator $(\cdot)$ in (5a) and (5b) represents differentiation.

Report Documentation Page

Form Approved
OMB No. 0704-0188

1. REPORT DATE	2. REPORT TYPE	3. DATES COVERED
14 APR 2005	**N/A**	**-**

4. TITLE AND SUBTITLE	5a. CONTRACT NUMBER
Mutually Dispersive Pulse Coding to Enhance Non-Linear Ambiguity Suppression	5b. GRANT NUMBER
	5c. PROGRAM ELEMENT NUMBER
6. AUTHOR(S)	5d. PROJECT NUMBER
	5e. TASK NUMBER
	5f. WORK UNIT NUMBER
7. PERFORMING ORGANIZATION NAME(S) AND ADDRESS(ES) **Department of Electrical and Computer Engineering Air Force Institute of Technology, Wright-Patterson AFB, OH, USA**	8. PERFORMING ORGANIZATION REPORT NUMBER
9. SPONSORING/MONITORING AGENCY NAME(S) AND ADDRESS(ES)	10. SPONSOR/MONITOR'S ACRONYM(S)
	11. SPONSOR/MONITOR'S REPORT NUMBER(S)

12. DISTRIBUTION/AVAILABILITY STATEMENT
Approved for public release, distribution unlimited

13. SUPPLEMENTARY NOTES
See also ADM001798, Proceedings of the International Conference on Radar (RADAR 2003) Held in Adelaide, Australia on 3-5 September 2003.

14. ABSTRACT

15. SUBJECT TERMS

16. SECURITY CLASSIFICATION OF:			17. LIMITATION OF ABSTRACT	18. NUMBER OF PAGES	19a. NAME OF RESPONSIBLE PERSON
a. REPORT	b. ABSTRACT	c. THIS PAGE			
unclassified	**unclassified**	**unclassified**	**UU**	**6**	

$$\sigma_{lk} \equiv \left[\int_{-\infty}^{\infty} t^2 |\rho_{lk}(t)|^2 dt\right]^{\frac{1}{2}} = \left[\frac{1}{2\pi}\int_{-\infty}^{\infty} |j\dot{P}_{lk}(\omega)|^2 d\omega\right]^{\frac{1}{2}} \quad (5a)$$

$$\sigma_{lk} = \left[\frac{1}{2\pi}\int_{-\infty}^{\infty} \dot{A}^2(\omega)d\omega + \frac{1}{2\pi}\int_{-\infty}^{\infty} (\dot{\Phi}_l - \dot{\Phi}_k)^2 A^2(\omega)d\omega\right]^{\frac{1}{2}} \quad (5b)$$

For $k = l$ in (5b), σ_{kk} represents the ACF rms time duration and is purely a function of envelope $A(\omega)$ (second term of second equation identically cancels). To achieve a maximally compressed ACF response, (5b) is made as small as possible; this provides the impetus for designing optimal envelope $A(\omega)$ such that the ACF rms time duration is minimized. Similarly, to achieve a large dispersed response, the CCF rms time duration, $k \neq l$ in (5b), is made as large as possible; the σ_{lk} dispersion has contributions due to both the envelope and the phase functions. With the envelope minimization constraint in place, the phase functions are designed to optimize the CCF rms duration.

Optimality in compression and mutual dispersion is achieved using the following process [4]:

1) For optimal compression, the envelope taper is derived by solving solution the following constrained optimization problem:

$$\begin{aligned} &\textit{Minimize} \quad \frac{1}{2\pi}\int_{-\infty}^{\infty} \dot{A}^2(\omega)d\omega \\ &\textit{Such that} \quad \frac{1}{2\pi}\int_{-\infty}^{\infty} A^2(\omega)d\omega = 1 \end{aligned} \quad (6)$$

Using calculus of variations, a cosine taper envelope of the following form may be derived:

$$A(\omega) = \sqrt{\frac{4\pi}{\Omega_0}}\cos\left(\frac{\pi\omega}{\Omega_0}\right) \qquad |\omega| \le \frac{\Omega_0}{2} \quad (7)$$

2) For M symbols, use any set of M maximally equidistant unit-vectors in M-Dimensional space (hermits), $\boldsymbol{C} = [\boldsymbol{c}_0\ \boldsymbol{c}_1\ \boldsymbol{c}_2\ \ldots\ \boldsymbol{c}_{M-1}]$. One solution to this hermit problem is defined as follows [4]:

$$\boldsymbol{C} = \frac{1}{\sqrt{M^2 - M}}\begin{bmatrix} M-1 & -1 & \cdots & -1 \\ -1 & M-1 & \cdots & -1 \\ -1 & -1 & \cdots & -1 \\ \vdots & \vdots & \ddots & \vdots \\ -1 & -1 & \cdots & M-1 \end{bmatrix}_{M\times M} \quad (8)$$

3) Choose any set of odd basis functions given by

$$\boldsymbol{\varphi}(\omega) = [\varphi_0(\omega)\ ,\ \varphi_1(\omega)\ ,\ \varphi_2(\omega)\ ,\ \ldots\ ,\ \varphi_{M-1}(\omega)]^{\mathrm{T}}$$

while satisfying windowed orthonormality given by:

$$\frac{1}{2\pi}\int \varphi_k(\omega)\varphi_l(\omega)A^2(\omega)d\omega = \delta_{kl} = \begin{cases} 1 & k = l \\ 0 & k \neq l \end{cases} \quad (9)$$

4) Describing M phase-rate functions as:

$$\dot{\Phi}_k(\omega) = \sqrt{G_D}\,c_k^T\boldsymbol{\varphi}(\omega)$$

where G_D is a dispersive gain factor, (dot represents differentiation) yields phase functions of the form:

$$\Phi_k(\omega) = \sqrt{G_D}\ \boldsymbol{c}_k^T \int_{\omega}\boldsymbol{\varphi}(\omega)d\omega \quad (10)$$

5) Resultant time and frequency domain expressions for mutually dispersive codes is expressed as:

$$\begin{aligned} f_k(t) &= \frac{1}{2\pi}\int_{-\Omega_0/2}^{\Omega_0/2}\sqrt{A(\omega)}\,e^{j[\omega t + \Phi_k(\omega)]}d\omega \\ F_k(\omega) &= \sqrt{A(\omega)}\,e^{j\Phi_k(\omega)} \end{aligned} \quad (11)$$

It can be shown that symbols designed with this process yield theoretical ACF and CCF rms time durations of:

$$\sigma_{kk} = \frac{\pi}{\Omega_o} \quad (12)$$

$$\sigma_{kl} = \left[\sigma_{kk}^2 + \frac{2M}{M-1}G_D\right]^{\frac{1}{2}} \quad (13)$$

Furthermore, these theoretical expectations are independent of basis selection provided the aforementioned process requirements are satisfied.

III. Symbol Synthesis

A closed-form expression for symbol $f_k(t)$ is generally unobtainable. Consequently, a rectangular-rule approximation to the inverse Fourier transform is considered, naturally enabling numerical methods for computational analysis. The l^{th} element of the k^{th} symbol, spectrally sampled at uniform intervals of ω_o, is given by

$$\widetilde{F}_k[l] = \sqrt{A(l\omega_o)}\,e^{j\Phi_k(l\omega_o)} = \widetilde{A}[l]\,e^{j\widetilde{\Phi}_k[l]} \quad (14)$$

The n^{th} element of the k^{th} symbol, temporally sampled at uniform intervals of t_o such that $t_o\omega_o = 2\pi/N_s$ where N_s is the number of samples, is given by

$$\begin{aligned} \widetilde{f}_k[n] &= \frac{1}{N_s}\sum_{l=0}^{N_s-1}\widetilde{F}_k[l]\,e^{j2\pi ln/N_s} \\ &= \frac{1}{N_s}\sum_{l=0}^{N_s-1}\widetilde{A}[l]\,e^{j\left(\widetilde{\Phi}_k[l] + 2\pi ln/N_s\right)} \end{aligned} \quad (15)$$

The sampled signals are further windowed in time to be realizable. Windowed symbol must contain at least 99.9% of the original energy.

IV. Basis Selection and Performance

To validate the symbol design theory and the associated metrics, two types of basis functions are used to generate a family of $M = 4$ symbols with intermediate frequency (IF) bandwidth of $\Omega_o = 2\pi \times 10^3$ rad/s (1.0 KHz) and dispersive gain $G_D = 10$.

A. Sinusoidal Basis

The family of sinusoidal functions is one obvious choice of basis functions due to their orthogonal properties. Using this family, the general form for each element in a set of sinusoidal basis functions is described as:

$$\varphi_n(\omega) = \sqrt{2}\, sin(a_n \omega) \tag{16}$$

where $a_k \in$ Integers, $a_k \neq a_l \; \forall \; k, l$ and bandwidth $\Omega_0 = 2m\pi$ for m, a positive integer. These constraints ensure compliance to the orthonormal requirement in (9). The symbols were constructed using the process outlined in (5) to (10). The correlation metrics of the synthesized symbols are summarized in Table I, including Peak Sidelobe Level (PSL), Integrated Sidelobe Level (ISL) and Peak Cross-Correlation Level (PCCL). The rms metrics of the symbols meet the theoretical expectation of (12) and (13) thus validating the symbol design theory. The autocorrelation sidelobe metrics, PSL and ISL, are characteristic of the cosine taper envelope and remain relatively constant with increased bandwidth, dispersive gain, and choice of other basis functions. However, the PCCL metric tends to change with dispersive gain, bandwidth and basis function selection. As dispersive gain increases, the PCCL metric improves and the signal time duration (to capture 99.9% energy) increases. Applications requiring shorter duration signals may not be able to use symbols generated with a large dispersive gain and benefit from lower PCCL levels. Thus, piecewise linear basis functions are introduced to "flatten" CCF sidelobes without the need to increase the dispersive gain to reduce PCCL's.

B. Piecewise Linear Basis

A set of orthonormal piecewise linear basis functions is generated with each element in this set defined as:

$$\begin{aligned}\varphi_n(\omega) = \beta_n \Bigg[& (\omega + \Omega_0/2)\, rect\left(\frac{\omega + \Omega_0/2 - \Omega_n/8}{\Omega_n/4}\right) \\ & + \sum_{m=0}^{2a_n-1} (-1)^m (\omega + \omega_m)\, rect\left(\frac{\omega - \omega_m}{\Omega_n/2}\right) \\ & + (\omega - \Omega_0/2)\, rect\left(\frac{\omega - \Omega_0/2 + \Omega_n/8}{\Omega_n/4}\right)\Bigg]\end{aligned} \tag{17}$$

$$\beta_n = \frac{4a_n\sqrt{3}}{\Omega_0} \quad , \quad \Omega_k = \frac{\Omega_0}{a_k} \quad , \quad \omega_n = \frac{\Omega_0(n/a_k - 1)}{2}$$

These basis functions are constructed to maintain orthonormality within a uniform taper rather than the optimal cosine taper; $A(\omega)$ in (9) is replaced with a uniform taper. However, the symbols are still synthesized with the cosine taper although the phase functions are designed for a uniform envelope. This "mismatch" is necessary to retain the desirable sidelobes characteristics of the cosine taper envelope. The ACF improvement comes at the cost of possible degradation in the rms metric of the CCF. The CCF metric will no longer adhere to (13) although (12) is still valid for the ACF. The correlation metrics are shown in Table I while the ACF and CCF results are shown Fig 1. The time function windowed at 99.9% of the energy is show in Fig 2. A comparison of Linear Frequency Modulated (LFM) symbols with equivalent time bandwidth product is also included to provide a measure of comparison.

V. NLAS Performance Demonstration

For concept demonstration, four uniquely coded, equal energy symbols were generated using the above piecewise basis. An *Unambiguous* input signal $s_U(t)$ was created using symbol $f_1(t)$ and random noise $n(t)$, as shown in (18), with powers adjusted to achieve a –20 dB signal-to-noise ratio (SNR). An *Ambiguous* input signal $s_A(t)$ was created by adding two symbols to $s_U(t)$ as shown in (19). The signal powers in $f_2(t)$ and $f_3(t)$ were adjusted to achieve a 0 dB SNR – the ambiguous signal powers are +20 dB above the unambiguous signal power. The remaining symbol $f_4(t)$ was used by the NLAS processor to generate the Adaptive Reserved Code Thresholds (ARCT) used for suppressing ambiguous signal responses [3].

$$s_U(t) = f_1(t) + n(t) \tag{18}$$

$$s_A(t) = s_U(t) + f_2(t) + f_3(t) \tag{19}$$

Unambiguous signal $s_U(t)$ is first input into the NLAS processor. Although there is no ambiguous energy to suppress in this case, the NLAS processor goes through all suppression operations and provides a "colored" baseline for performance comparison. Ambiguous signal $s_A(t)$ is then input into the NLAS processor and produces a final output as shown in Fig. 4. A representative focusing and suppression operation for one of the undesired ambiguous input signals is shown in Fig. 3. As illustrated, all data points exceeding the ARCT (dashed line) are zeroed out prior to subsequent processing [3]. The final NLAS output response of Fig. 4 is nearly identical to the "colored" response obtained from the unambiguous signal input case– if complete suppression of $f_2(t)$ and $f_3(t)$ occurs, the suppressed response would be identical to the "colored" response. Despite the presence of ambiguous responses that were +20 dB higher than the response of interest, the NLAS processor output permits reliable signal detection.

VI. CONCLUSION

Sinusoidal basis functions provide a means for generating optimal mutually dispersive symbols, with dispersive gain providing control over crosscorrelation dispersion. The sinusoidal basis achieves theoretical autocorrelation and crosscorrelation performance, in terms of rms time duration, demonstrating the validity of the proposed theorem. If the envelope optimality constraint is relaxed during phase functions design, piecewise linear basis functions provide improved performance in terms of cross correlation sidelobes with minimal impact on the rms metric.

The theory of designing mutually dispersive symbols and the resultant generation process using sinusoidal bases provides a reliable method for generating M mutually dispersive symbols, with bandwidth Ω_o controlling autocorrelation compression and dispersive gain G_D controlling crosscorrelation dispersion. Although the correlation rms metrics are invariant to basis function selection, sidelobe characteristics of the auto- and cross-correlation functions are dependent upon the choice of envelope, basis functions, bandwidth and dispersive gain.

Using the proposed symbol design process and piecewise basis functions, the ambiguity suppression capability of a NLAS process was demonstrated. Despite the presence of two ambiguous signal responses that were +20 dB higher than the response of interest, the NLAS process yielded an output that clearly provides for reliable signal detection.

"The views expressed in this article are those of the author(s) and do not reflect the official policy or position of the United States Air Force, Department of Defense, or the US Government."

REFERENCES

[1] Palermo, Leith, and Horgen, Ambiguity Suppression By Nonlinear Processing, Eighth Annual Radar Symposium Record, June 1962.

[2] Anderson, J.M., Temple, M.A., Brown, W.M., and Crossley, B.L., "A Nonlinear Suppression Technique for Range Ambiguity Resolution in Pulse Doppler Radars," Proceedings of the 2001 IEEE Radar Conference, Atlanta, Georgia, May 2001, pp 141-146

[3] Anderson, J M. *Nonlinear Suppression of Range Ambiguity in Pulse Doppler.* PhD dissertation, Air Force Institute of Technology (AETC), 2001 (ADA397364)

[4] Papaphotis, M.J., *An Analysis of Mutually Dispersive Brown Symbols for Non-Linear Ambiguity Suppression*. M.S Thesis, Air Force Institute of Technology (AETC), 2002 (ADA401636)

[5] Rihaczek, A.W., *Principles of High-Resolution Radar*, New York: McGraw-Hill, 1969.

Table I Performance Metric Comparison

		PSL (dB)	ISL (dB)	PCCL (dB)	σ_{kk}	σ_{kl}
SINUSOIDAL	$\rho_{00}(\tau)$	-23.01	-18.85	- - - - -	$5.0\text{x}10^{-4}$	- - - - -
	$\rho_{11}(\tau)$	-23.01	-18.85	- - - - -	$5.0\text{x}10^{-4}$	- - - - -
	$\rho_{22}(\tau)$	-23.01	-18.85	- - - - -	- - - - -	- - - - -
	$\rho_{33}(\tau)$	-23.01	-18.85	- - - - -	- - - - -	- - - - -
	$\rho_{01}(\tau)$	- - - - -	- - - - -	-0.526	- - - - -	5.16
	$\rho_{02}(\tau)$	- - - - -	- - - - -	-0.456	- - - - -	5.16
	$\rho_{03}(\tau)$	- - - - -	- - - - -	-0.420	- - - - -	5.16
PIECEWISE	$\rho_{00}(\tau)$	-23.01	-18.95	- - - - -	$5.0\text{x}10^{-4}$	- - - - -
	$\rho_{11}(\tau)$	-23.01	-18.95	- - - - -	$5.0\text{x}10^{-4}$	- - - - -
	$\rho_{22}(\tau)$	-23.01	-18.95	- - - - -	$5.0\text{x}10^{-4}$	- - - - -
	$\rho_{33}(\tau)$	-23.01	-18.95	- - - - -	$5.0\text{x}10^{-4}$	- - - - -
	$\rho_{01}(\tau)$	- - - - -	- - - - -	-34.02	- - - - -	3.78
	$\rho_{02}(\tau)$	- - - - -	- - - - -	-32.50	- - - - -	5.25
	$\rho_{03}(\tau)$	- - - - -	- - - - -	-32.02	- - - - -	5.17
LFM	$\rho_{00}(\tau)$	-13.27	-7.11	- - - - -	$3.2\text{x}10^{-1}$	- - - - -
	$\rho_{11}(\tau)$	-13.27	-7.11	- - - - -	$3.2\text{x}10^{-1}$	- - - - -
	$\rho_{01}(\tau)$	- - - - -	- - - - -	-43.98	- - - - -	6.92

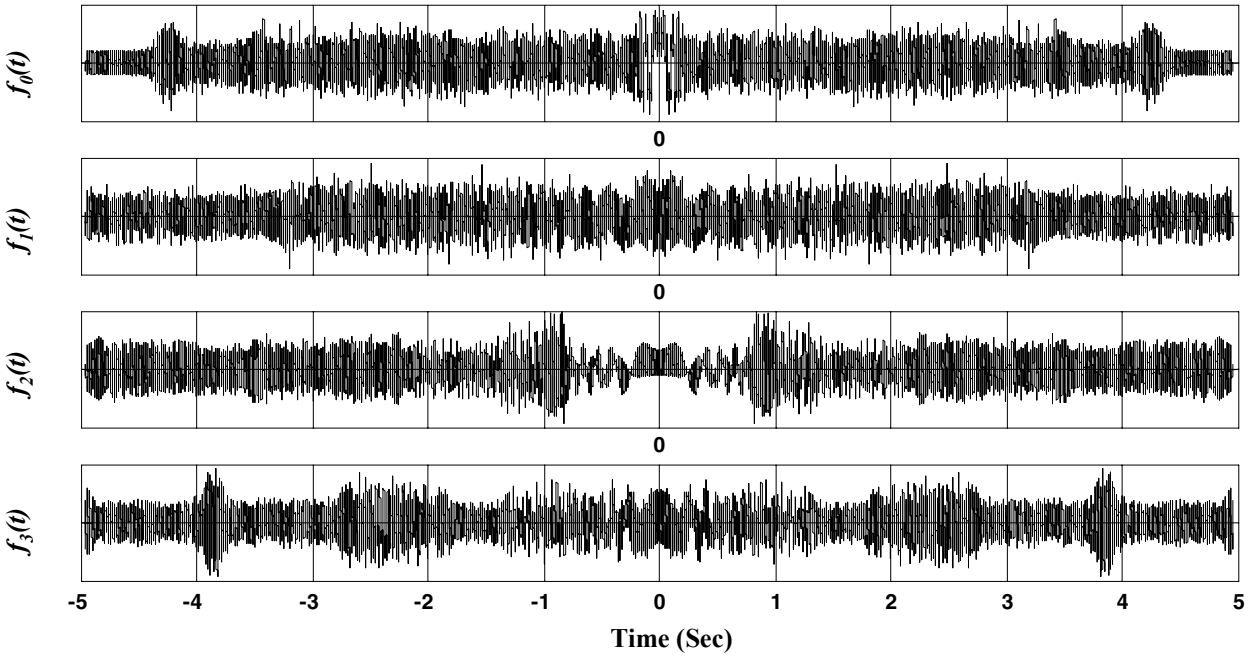

Figure 1. Piecewise Basis Time Response [Real Part]

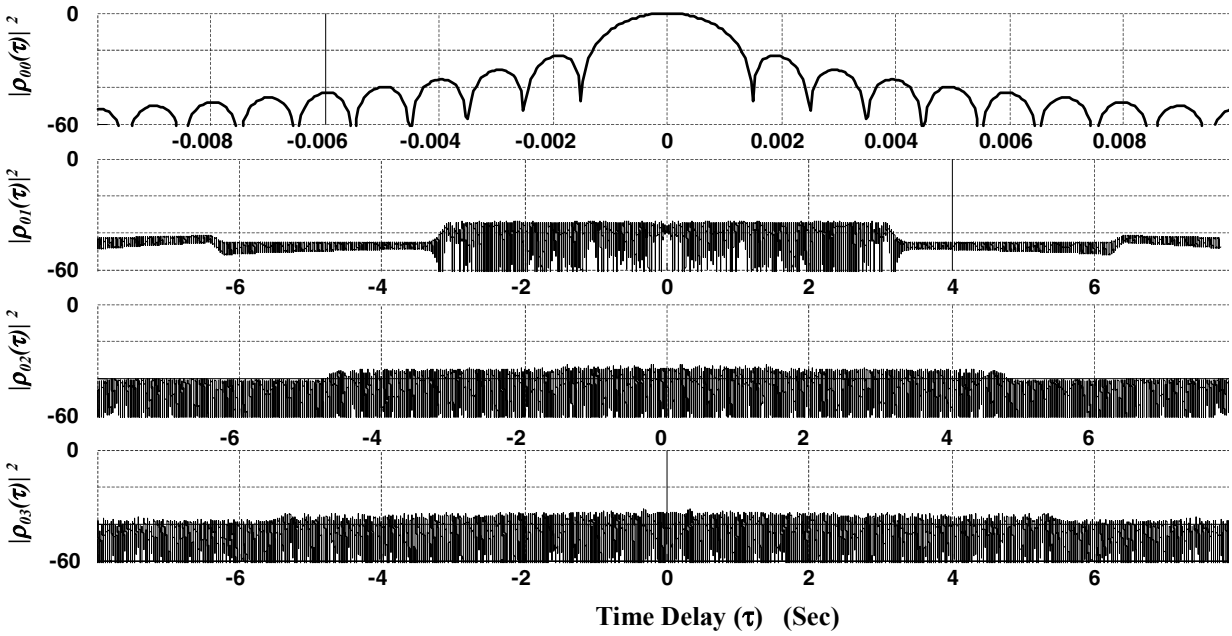

Figure 2. Piecewise Basis: Correlation Responses (dB)

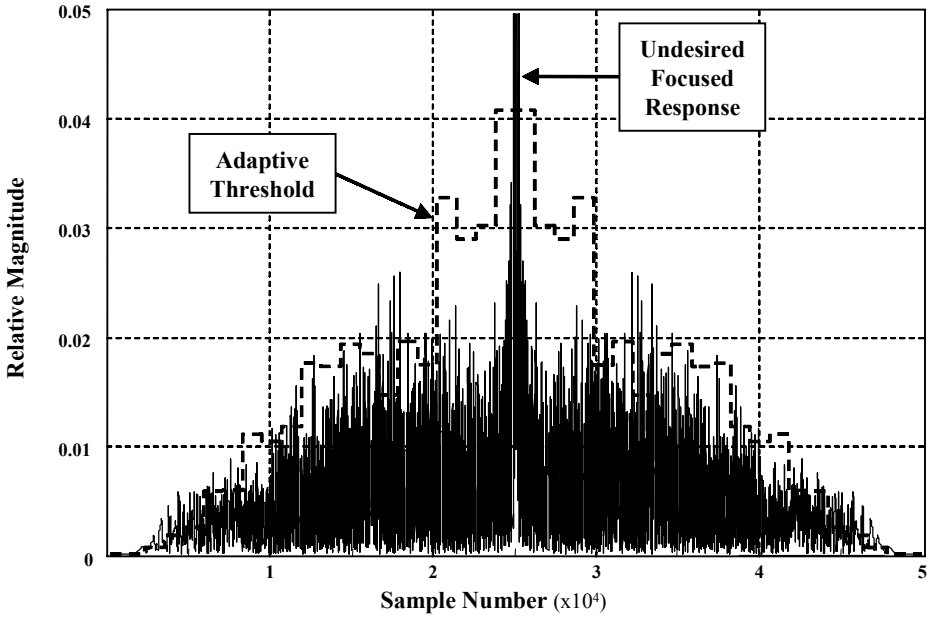

Figure 3. NLAS Suppression: 1st Stage Adaptive Reserved Code Thresholding

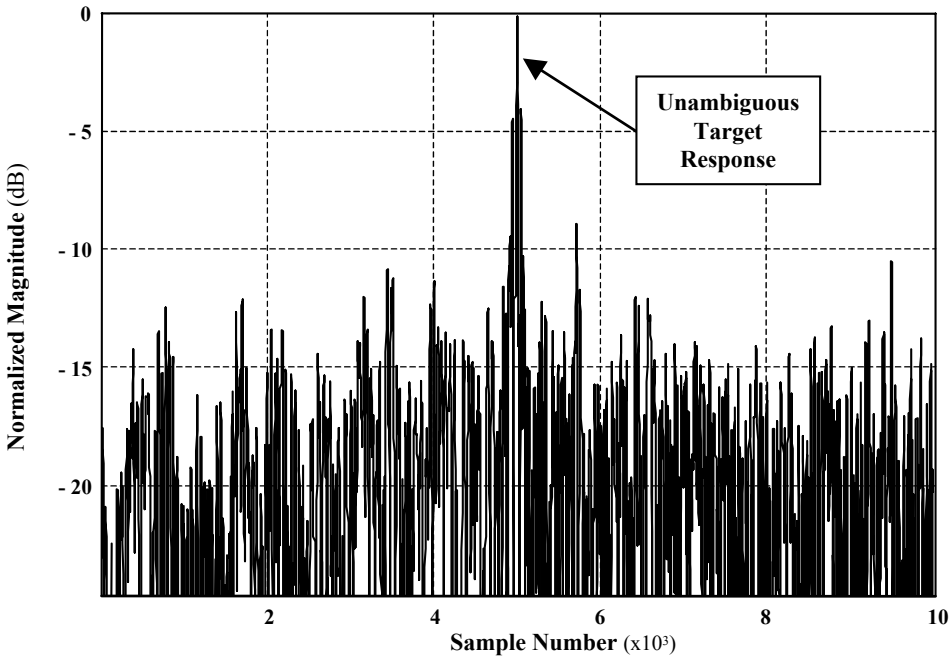

Figure 4. NLAS Output: *Ambiguous* Input Data